

PROCESSES OF NONCONSUMABLE ELECTRODE WELDING WITH WELDING CURRENT MODULATION (Review).

Part 1. Peculiarities of burning of nonstationary arcs with refractory cathode

U. BOI¹ and I.V. KRIVTSUN²

¹Guangdong Institute of Welding (China-Ukraine E.O. Paton Institute of Welding)
363 Chiansin Str., Tianhe, 510650, Guangzhou. E-mail: wuby@gwi.gd.cn

²E.O. Paton Electric Welding Institute of the NAS of Ukraine
11 Kazymyr Malevych Str., 03150, Kyiv, Ukraine. E-mail: office@paton.kiev.ua

Works devoted to the processes of inert-gas nonconsumable electrode welding with current modulation were reviewed. In the first part of the review attention is focused on studies, dealing with the features of running of thermal, gas-dynamic and electromagnetic processes in nonstationary arcs with refractory cathode at different modes of arc current modulation. 35 Ref., 2 Tables, 18 Figures.

Keywords: arc with refractory cathode, arc plasma, TIG welding, welding current modulation, pulse, frequency, fill factor, amplitude

Inert-gas nonconsumable electrode arc welding (TIG) now is one of the main technological processes for producing high-quality permanent joints of critical structures from steels, titanium and aluminium alloys [1]. At the same time, this welding process does not meet the ever increasing requirements of modern industrial production, because of low penetrability of the welding arc with the refractory cathode and low process efficiency (welding speed). Therefore, over the last decades the efforts of scientists and specialists have been aimed at improvement of the effectiveness of TIG welding at preservation of the high quality of welds.

Modulation of welding current in TIG welding is one of the most widely applied methods to control the thermal, gas-dynamic and electromagnetic characteristics of the arc, as well as the characteristics of its thermal and dynamic (force) impact on the metal being welded. Variation of current modulation parameters, such as frequency, relative pulse duration, amplitude and shape, allows controlling in a rather wide range the depth and shape of metal penetration, thermal cycle of welding, and, therefore, affecting the structure and properties of the metal of the weld and HAZ.

Many studies are devoted to investigation of the processes of TIG welding with arc current modulation [2–32]. Modes with low-frequency (modulation frequency $f \leq 50$ Hz) [3, 5, 6, 8, 9, 11, 15, 25, 30], medium-frequency ($f \sim 5$ kHz) [2, 4–9, 15, 17] and high-frequency ($f > 10$ kHz) [2, 5, 6, 10, 13–15, 17,

20–24, 27–29] with pulse current modulation were experimentally studied. Works [7, 11, 12, 16, 18, 19, 24, 26–29, 31, 32] are devoted to theoretical study and mathematical modeling of TIG welding by modulated current. Let us consider the results of investigations, described in the above works in greater detail. Here, in the first part of this review we will focus on the works devoted to experimental studies of physical processes in nonstationary arcs with refractory cathode in different modes of arc current modulation.

In TIG welding with welding current modulation the processes of transfer of energy, pulse, mass and charge in arc column plasma are nonstationary, that is due to the change of energy, gas-dynamic and electromagnetic characteristics of arc plasma under the impact of periodically changing current. As a result, the distributed and integral characteristics of plasma of a nonstationary welding arc, as well as characteristics of its impact on the metal being welded, can differ considerably from the respective characteristics for direct current arcs (at other conditions being equal), the degree of this difference depending on pulse repetition rate and shape fill factor, modulation amplitude and other factors.

Based on experimental data of works [21–23] of Chinese scientists, the effective value of voltage of a 3 mm arc with a refractory cathode ($W = 2\% \text{ Ce}$) of 2.4 mm diameter increases practically in proportion to current modulation frequency in welding 6 mm stainless steel 0Cr18Ni9Ti in argon (welding speed of 120 mm/min), as shown in Figure 1. In these experiments, the following parameters of pulse modulation

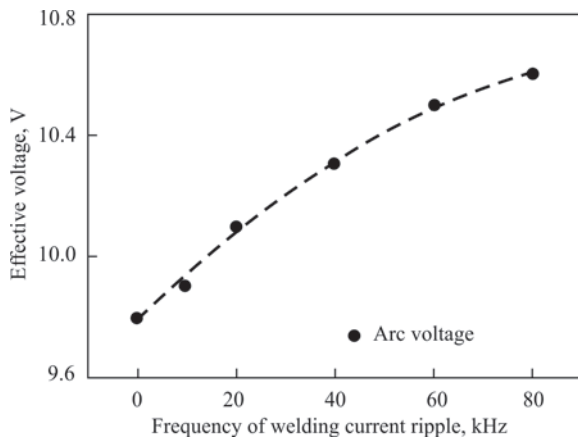


Figure 1. Dependence of effective value of arc voltage on welding current modulation frequency [22]

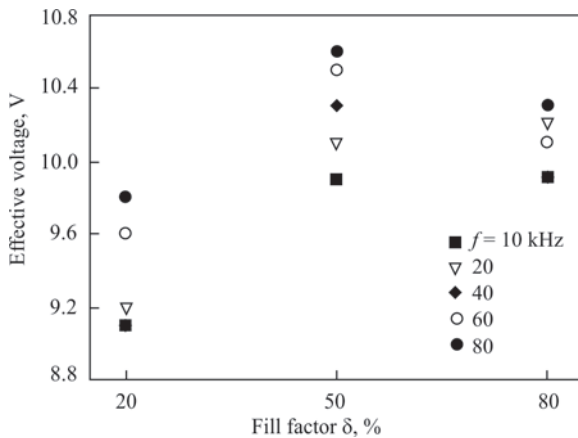


Figure 2. Effective values of arc voltage at different frequencies of current modulation, depending on fill factor [21, 22]

of current were used: square wave pulses, repetition rate f was varied in the range of 10–80 kHz, base current $I_b = 50$ A, pulse current $I_p = 130$ A, effective current value

$$I_{\text{eff}} = \sqrt{(1-\delta)I_b^2 + \delta I_p^2} = 98.5 \text{ A,}$$

where δ is the fill factor, determined as the ratio of pulse duration to modulation period (in the considered case $\delta = 0.5$). The respective experiment on direct current welding was conducted at $I = 100$ A that practically coincides with effective value of modulated current.

Table 1. Parameters of the studied mode of HFP modulation of arc current [21, 22]

Mode number	δ , %	f , kHz	I_{eff} , A	I_b , A	I_p , A
1	20	10–80	89.4	60	160
2	50	10–80	98.5	50	130
3	80	10–80	96.0	45	105

The effect of fill factor δ on effective value of arc voltage at TIG welding of stainless steel with high-frequency pulse (HFP) modulation of current was investigated in [21, 22]. Three modes of pulse modulation were studied, the parameters of which are summarized in Table 1.

Results of measurement of the respective values of arc current are shown in Figure 2. As follows from experimental data, given in this Figure, with δ increase the effective value of arc voltage first rises, and then remains practically constant in the frequency range of 10–20 kHz and somewhat decreases at $f > 40$ kHz. This weakens the impact of frequency on effective value of voltage and high values of the fill factor.

A marked reduction of transverse dimensions of the column of the arc with a refractory cathode at increase of modulation frequency, illustrated in Figure 3, was noted in works [21–23], by comparing the images of arc plasma at different values of current modulation frequency.

Obtained data allowed the authors performing quantitative evaluation of the force acting on the surface of metal being welded, the values of which are given in Table 2, and are indicative of increase of the above force with increase of modulation frequency f and fill factor δ .

Work [8] is an experimental study of a 3 mm non-stationary argon arc with a 2 mm refractory cathode (W + 2 % Th) burning in the frequency range of current modulation from 0.05 Hz (practically constant current) up to 5 kHz. The anode used was a copper water-cooled plate or sample from SUS 304 stainless steel 3 mm thick (in the latter case the arc moved relative to the sample at a constant speed equal to 1.6 mm/s). Pulse modulation of current was performed in the range from base current value $I_b = 10$ A

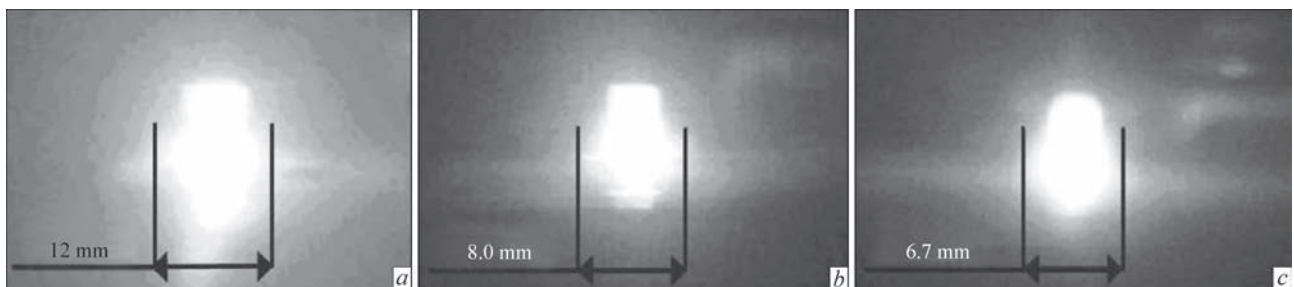


Figure 3. Photographs of the column of an arc at direct current (a) and at HFP modulation of current with the frequency of 20 (b) and 80 (c) kHz ($\delta = 20$ %) [22, 23]

up to maximum value $I_p = 150$ A. Two pulse shapes were used: rectangular (square wave) and triangular (without pauses).

During the experiment it was found that the dynamic characteristics of the considered arc depend on the frequency and shape of current pulses, as well as anode material. In particular, at low frequencies ($f < 1$ Hz), change of arc voltage occurs practically along the static volt-ampere characteristic (VAC) of the arc. For frequencies of 1–10 Hz, even under the condition that the respective values of DC arc voltage for the base and maximum current values differ, the arcing voltage is practically constant with typical increase and decrease of instantaneous values at the moments of current rise and drop, respectively. The latter effect is observed, if the speed of current change at the pulse fronts exceeds the value of $1.5 \cdot 10^5$ A/s and is attributed by the authors of [8] to delaying of the change in concentration of the charged particles, and, accordingly, of electrical conductivity of arc plasma at an abrupt rise and drop of current. In the range of modulation frequencies of 100 Hz – 1 kHz the average arc voltage decreases at base value of current and somewhat increases at peak value of current. Finally, at frequencies above 2.5 kHz the arc behaves as an element of a circuit with constant ohmic resistance.

Dependencies of voltage V of the arc with a copper (water-cooled) and steel (consumable) anode at base $V_b = V(I_b)$ and peak $V_p = V(I_p)$ current values on modulation frequency are shown in Figure 4. As follows from experimental data presented in this Figure, average value of arc voltage markedly decreases at base current value, whereas the respective value of voltage in the current pulse somewhat increases with increase of frequency. This allowed the authors of [8] to conclude that the average arc power has maximum value at small values of f (actually for a DC arc) and decreases with increase of modulation frequency. So, for instance, the average arc power at 2.5 kHz frequency, in the authors' estimates, is equal to just 70 % of the respective value at $f = 0.5$ Hz.

Work [5] is also devoted to investigations of the dynamic characteristics of free-burning and constricted (plasma) arc with a refractory cathode and copper water-cooled anode, burning in argon at direct current in the range of 20–250 A. In this work experimental frequency characteristics were used to check the applicability of the differential equation of arc dynamics, which was derived on the base of the channel model:

$$\theta \frac{dU}{dt} + U = \theta R_s \frac{di}{dt} + R_d i, \quad (1)$$

where $R_s = U_0/I_0$ and $R_d = dU/dI$ are the static and dynamic resistance of the arc, respectively; θ is the

Table 2. Force acting on the welded metal surface (mN) at different parameters of pulse modulation of arc current [22]

f , kHz	δ , %		
	20	50	80
0 (direct current)	3.1	3.1	3.1
10	5.9	9.6	4.9
20	6.5	9.2	5.0
40	9.1	11.8	4.4
60	11.6	16.0	5.3
80	17.6	17.1	4.4

arc time constant, determining the change of arc column conductivity G at a jumplike change of current

$$\frac{1}{\theta} = - \frac{d \ln G}{dt}$$

Current modulation in the experiments was performed by superposition on direct current of a variable (sinusoidal) component with 4 A amplitude and frequency in the range from 20 Hz up to 160 kHz. It was found that for a constricted arc (tungsten electrode diameter, plasmaforming nozzle diameter and electrode insertion into the nozzle were equal to 4 mm, electrode spacing was 11 mm, plasma gas flow rate varied in the range from 0.055 up to 0.17 g/s) the arc time constant decreases from 50 to 15 μ m with increase of current and plasma gas flow rate that qualitatively and quantitatively coincides with the results of calculations for currents above 50 A. As regards

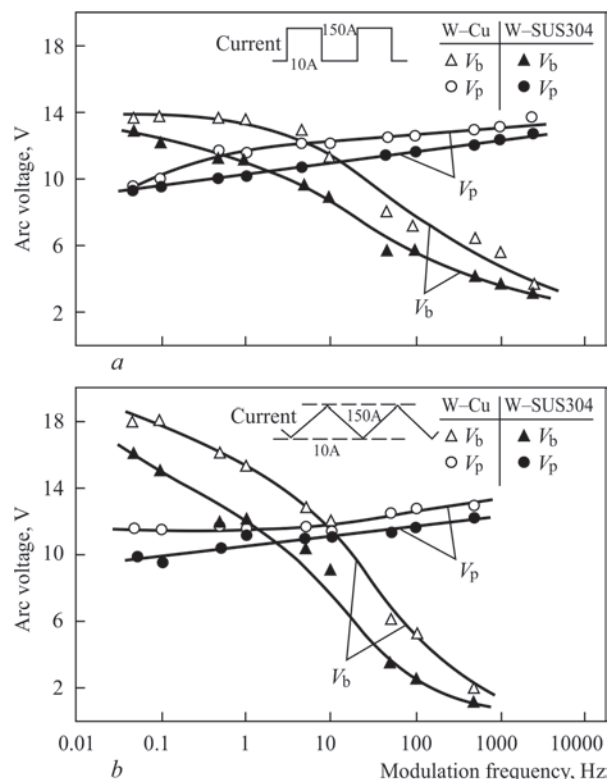


Figure 4. Arc voltage V_b (at base) and V_p (at peak values of current), depending on its pulse modulation frequency: a — rectangular pulses (average values of V_b and V_p); b — triangular pulses (maximum values of V_b and V_p) [8]

free-burning argon arc (cathode diameter of 4 mm, arc length of 2–6 mm), experimentally determined frequency characteristics of the arc differ from the calculated ones both in the area of low and high frequencies. In particular, calculation of the time constant for a 2 mm arc yields the values of 2–14 μ s, and unlike the constricted arc, greater θ values correspond to greater current values. Analysis of the obtained data led the authors of [5] to the conclusion that the channel model of the arc, used to derive equation (1), is too simplified for description of a free-burning arc in argon and at analysis of its dynamics, it is necessary to take into account heat transfer due to convection, as well as energy losses for radiation.

In work [9] results of experimental studies of the optical and electrical characteristics of the arc with a refractory cathode, burning both at direct current and at its modulation, are described. Electric arc with a tungsten (W + 2 % Th) cathode of 2.38 mm diameter and 30° sharpening angle of the working end was used in the experiments, and shielding gas (Ar) was fed through a nozzle of 9.5 mm diameter. The arc was powered from a source, which provided direct current in the range from 0 up to 300 A, and to which a transistor regulator was connected for modulation of current with up to 3000 Hz frequency at different shape of the pulses. A copper water-cooled anode (solid and split with 0.075 mm width of the gap) or an anode from stainless steel 304 of 22.22 mm diameter and 7.62 mm thickness, soldered into a copper water-cooled holder, were used. A photodiode array, containing 256 elements and operating in a wide range of wave lengths (400–1200 nm) was applied to measure the intensity of arc radiation. A lens and a diaphragm were used to focus the arc radiation on the array surface, after passing through a light filter, preventing photodiode saturation by high intensity radiation. The optical system was tuned to measure the distribution of radiation intensity in a plane, located at the distance of 0.01 mm from the anode surface.

Experiments on measurement of radiation intensity of DC arc (in the range of 50–300 A), of length

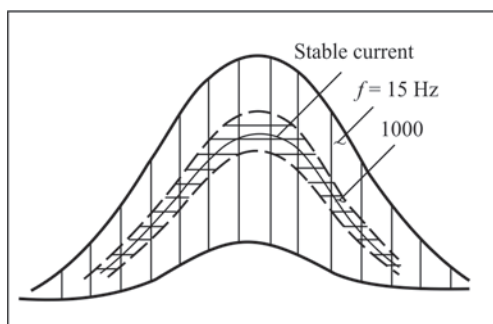


Figure 5. Typical shapes of a signal from photodiode array, characterizing arc radiation intensity distribution [9]

from 2.0 mm up to 6.3 mm, showed that in the immediate vicinity of the anode surface the distribution data can be approximated with sufficient accuracy by the respective Gaussian curve

$$\varphi(x) = \varphi_0 \exp\left(-\frac{x^2}{2\sigma^2}\right), \quad (2)$$

where x is the distance from the plane passing through the axis of symmetry of the arc ($x = 0$), and distribution parameter σ is defined as the distance, at which the value of the function is equal to 60 % of the respective value of φ_0 in the above plane. Processing of experimental data for an arc of 4 mm length yielded σ values increasing with arc current rise from 1.0 mm at $I = 50$ A up to 2.4 mm at $I = 300$ A and independent on the used anode type (copper water-cooled or steel) within the measurement error.

In the case of sinusoidal modulation of arc current in the range of 30–270 A (average current value $\langle I \rangle = 150$ A) the measured distribution of arc radiation intensity essentially depends on modulation frequency, as shown in Figure 5. So, at small values of f , the corresponding distribution periodically changes with the frequency equal to the selected modulation frequency between the distribution of radiation intensity of a DC arc at $I = I_{\min} = 30$ A and its distribution for an arc at $I = I_{\max} = 270$ A. Such behaviour is preserved right up to the frequency of the order of 500 Hz. With increase of modulation frequency the amplitude of the above changes decreases and at $f > 1000$ Hz the distribution of radiation intensity of an arc of modulated current behaves similar to the distribution for a DC arc at $I = \langle I \rangle = 150$ A.

In work [9] an experimental determination of the density of electric current on the anode surface was also performed. A split anode procedure was used, described in detail in [33], and it was assumed that the anode current density has Gaussian distribution along the radius, similar to (2). It is established that the thus determined values of the parameter of σ distribution for a direct current arc, increase with the increase of current and arc length. Comparison of the obtained values of the parameter of radial distribution of current density on the anode with the respective σ values for a linear distribution of radiation intensity showed that the above values practically coincide for arcs of length from 2.0 up to 6.3 mm in the current range of 50–300 A. This allowed the authors to conclude that at the change of current (also due to modulation) and length of the arc, the transverse size of the current channel on the anode surface with a sufficiently high degree of accuracy follows the respective changes of the transverse size of distribution of its radiation in-

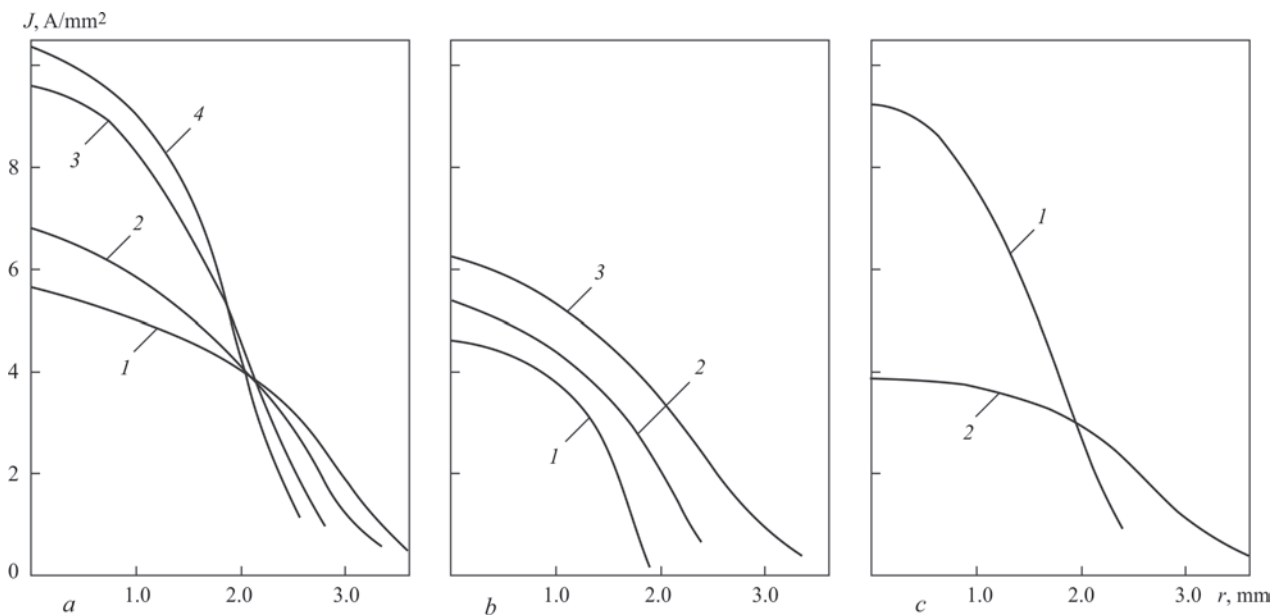


Figure 6. Radial distributions of average over the modulation period values of electric current density on the anode surface: *a* — $\langle I \rangle = 100$ A; $L = 4$ mm (*1* — direct current; *2* — $f = 5$; *3* — 10 ; *4* — 20 kHz); *b* — $f = 5$ kHz, $L = 2$ mm (*1* — $\langle I \rangle = 30$; *2* — 50 ; *3* — 100 A); *c* — $\langle I \rangle = 100$ A; $f = 10$ kHz (*1* — $L = 4$; *2* — 8 mm) [10]

tensity. Thus, a simpler and faster method of measuring the arc radiation intensity can be used instead of the experimental determination (by split anode method) of the distribution of anode current density.

Here, it should be noted that the assumption of Gaussian distribution of density of anode current of the arc, used by the authors [9], is insufficiently substantiated. From the viewpoint of theory, the most theoretically sound is the approach based on solution of Abel integral equation. Here, the task of restoration of current density distribution in the arc anode region is mathematically incorrect and requires development of stable algorithms for processing the experimental data, obtained using a split anode. In [34], a new procedure was proposed for restoration of density of anode current, based on application of a stable method of numerical calculation of the second derivative from experimentally measured discrete function of arc current distribution through the split anode sections.

Work [10] is devoted to experimental study of distributions of average values of current density and pressure of the arc on the anode surface at high-frequency pulse modulation of current. All the experiments were conducted with application of an electric arc with tungsten (cerium-activated) cathode of 3 mm diameter with 60° angle of working end sharpening. The shielding gas used was argon, fed through a nozzle of 10 mm diameter with the flow rate of 12 l/min. The arc anode was copper water-cooled one with 1.0 mm orifice for measuring the arc pressure and current density (in the latter case an insulated tungsten probe of 0.9 mm diameter was inserted into the above orifice). Arc length L was varied in the range

of 2–8 mm, arc current modulation was performed by square-wave pulses (meander) without base with repetition rate f of up to 20 kHz, average current $\langle I \rangle$ was assigned in the range of 30 to 130 A.

Results of experimental measurement of radial distributions of time-averaged values of electric current density and arc pressure on the anode surface are given in Figures 6, 7. As follows from the curves given in these Figures, the average value of current density in the center of the region of anode binding of the arc rises with increase of modulation frequency (see Figure 6, *a*), as well as average current value (see Figure 6, *b*) and, contrarily, decreases with increase of arc length (see Figure 6, *c*).

As regards the distributions of average value of arc pressure, its value in the center of area of anode binding of the arc, by the data of [10], changes nonmonotonically with increase of current modulation frequency. In the frequency range from 0 to 5 kHz, the above value grows, whereas at further increase of frequency up to 20 kHz, the maximum value of arc pressure on the anode surface decreases noticeably (see Figure 7, *a*). Experimentally measured pressure in the center of anode binding of the arc at modulation frequency $f = 10$ kHz rises with increase of average current (see Figure 7, *b*) and decreases at increase of arc length (see Figure 7, *c*).

On the whole, experimental data obtained in work [10], allowed the authors to make a conclusion about contraction (reduction of the transverse size) of the anode region of the arc with the refractory cathode at pulse modulation of current. Here, the degree of such a contraction rises with increases of frequency

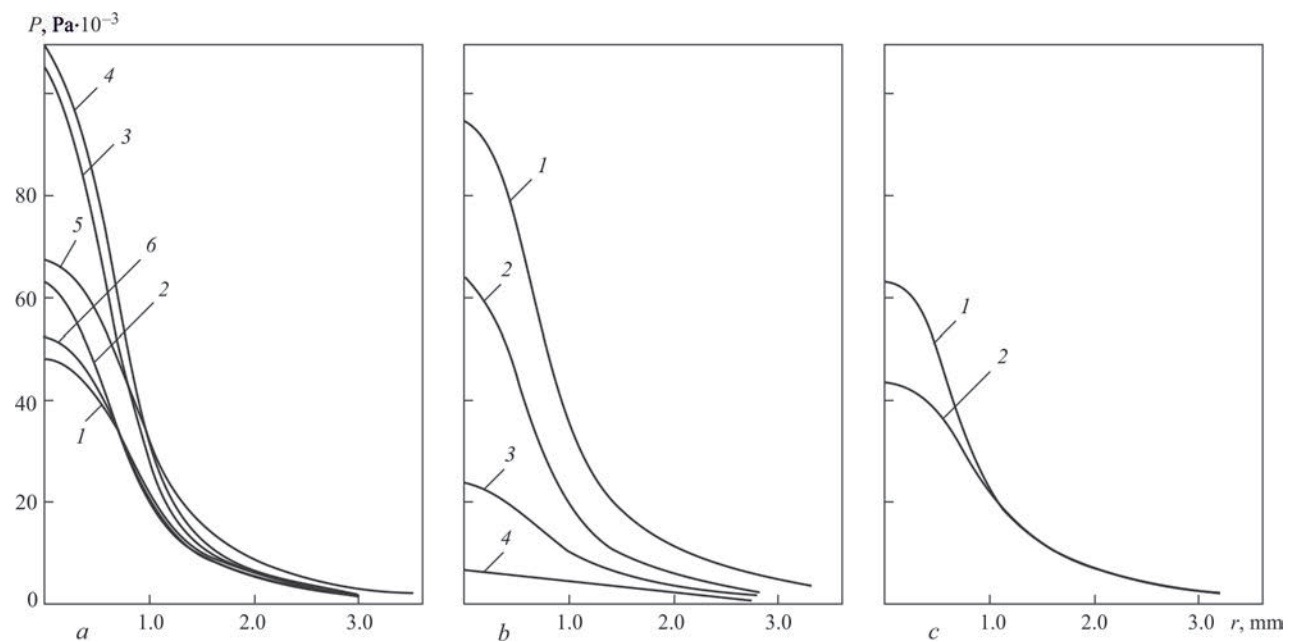


Figure 7. Radial distributions of arc pressures on the anode surface average over the modulation period: *a* — $\langle I \rangle = 100\text{ A}$; $L = 4\text{ mm}$ (I — direct current; 2 — $f = 300$; 3 — 3; 4 — 5; 5 — 10; 6 — 20 kHz); *b* — $f = 10\text{ kHz}$, $L = 4\text{ mm}$ (I — $\langle I \rangle = 130$; 2 — 100; 3 — 70; 4 — 40 A); *c* — $\langle I \rangle = 100\text{ A}$; $f = 10\text{ kHz}$ (I — $L = 2$; 2 — 6 mm) [10]

from 0 up to 5 kHz and decreases in the range from 5 to 20 kHz. The latter circumstance allows recommending the TIG process with HFP modulation of arc current for welding thin metals, using modulation frequency of the order of 20 kHz.

Completing consideration of work [10], it should be noted that the data given in report [13], disprove the regularity found by authors of [10], and consisting in increase of arc pressure on the anode surface with increase of current modulation frequency in the range of 0–5 kHz and its decrease at further frequency rise. In particular, the dependence given in Figure 8 is indicative of a continuous increase of the above value with increase of modulation frequency — quite fast in the range from 0 up to 5 kHz and slower at $f > 5\text{ kHz}$.

In work [14], the developed by the authors specialized power source ensuring HFP modulation of cur-

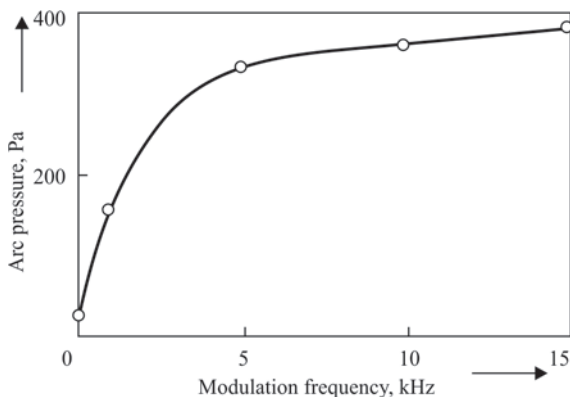


Figure 8. Arc pressure on the anode surface as a function of current modulation frequency: 2 mm arc with a refractory (W + 2 % Th) cathode of 2.4 mm diameter; sharpening angle of 60°, average current of 50 A; amplitude value of current of 150 A; pause current of 5 A [13]

rent with up to 20 kHz frequency at high peak values of current (up to 500 A), was used to experimentally study the influence of modulation parameters on the degree of contraction of an arc with the refractory cathode, arc pressure distribution over the anode surface, as well as its arcing stability. Experimental stands shown schematically in Figure 9, were used for determination of the above characteristics of the arc. The current shape realized in the experiments for two characteristic values of modulation frequency, is shown in Figure 10. Here, its value I_p in the pulse was equal to 500 A, and average current $\langle I \rangle$ had a constant value, equal to 150 A.

Results of the conducted experiments showed that arc pressure in the center of the region of anode binding of the arc rises continuously with increase of modulation frequency (at preservation of values $\langle I \rangle$, I_p), as shown in Figure 11. In particular, for a 2 mm arc at $f = 15\text{ kHz}$ the above value is two times higher than

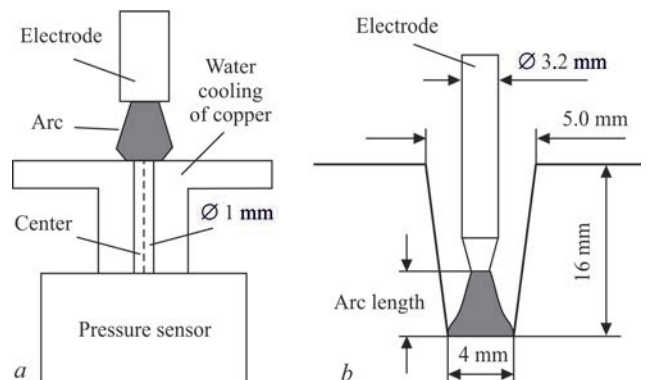


Figure 9. Diagrams of experimental stands for measurement of the pressure of an arc with a refractory cathode (*a*) and determination of its arcing stability (*b*) [14]

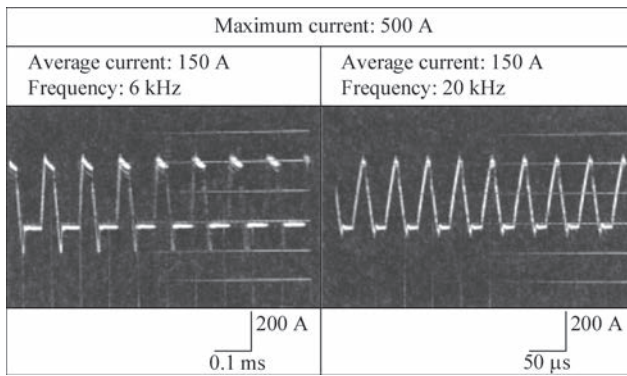


Figure 10. Characteristic shapes of arc current at different values of modulation frequency [14]

the respective value at $f = 5$ kHz, and three times higher than that for an arc of direct current equal to $\langle I \rangle$.

The photos of the arc at smaller average current ($\langle I \rangle = 50$ A) given in Figure 12, allowed the authors of [14] to conclude that the degree of arc contraction and its arcing stability at HFP modulation of current ($f = 10$ kHz) are higher than for the respective DC arc. In their opinion, this is related to the fact that the luminous area of the arc column at high-frequency modulation of current is essentially longer, compared to the respective area in DC arc, and it takes up the entire discharge gap. Experimental studies of the arc behaviour in a narrow groove, shown in Figure 9, *b*, confirmed the conclusion about a higher spatial stability of the arc with HFP modulation of current. So, the arc at modulation frequency $f = 10$ kHz was stable at length L of up to 5 mm, whereas DC arc had deviations even at $L = 2$ mm.

Work [15] is devoted to experimental investigation of physical characteristics of arc plasma at pulse modulation of current of an arc with the refractory cathode. Experiments were performed using an arc with a refractory cathode (W + 2% Ce) of 3 mm diameter, angle of working end sharpening of 60° , arc length of 4 mm, and shielding gas was argon. Selected as the arc power source was a batch-produced welding machine EWM Tetrix 500 with a special device connected to it, which ensured arc current modulation by rectangular pulses, in the frequency range up to 80 kHz. Pulse

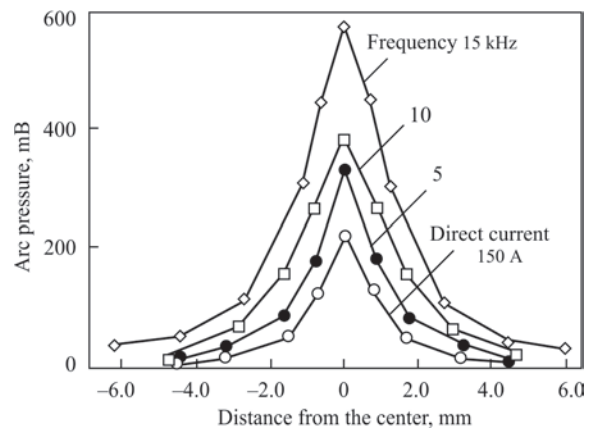


Figure 11. Distribution of arc pressure along the anode surface (relative units) at different values of current modulation frequency: maximum current — 500 A; average current — 150 A; arc length — 2 mm [14]

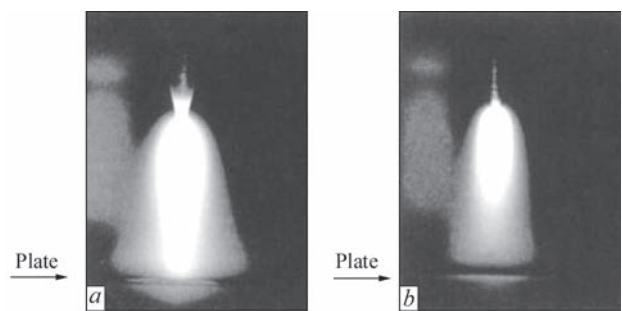


Figure 12. Appearance of an arc with HFP modulation of current (*a*) and DC arc (*b*), equal to $\langle I \rangle$ for *a*: frequency — 10 kHz; maximum current — 500 A; average current — 50 A; for *b*: direct current — 50 A [14]

current I_p was set to be equal to 100 A, base current I_b was assigned on the level of 50 A.

Figure 13 gives photos of the arc during a current pulse and at base current for different values of modulation frequency f . As follows from this Figure, with f increase the arc column shape changes from pear shape with diffuse binding to the anode to a spherical shape with a dark space near the anode. Here, for frequencies above 50 Hz, the appearance of the arc during the current pulse practically does differ from its shape during the pause.

Presented in Figure 14 dependencies of arc voltage at peak value of current $U_p = U(I_p)$ and at its base

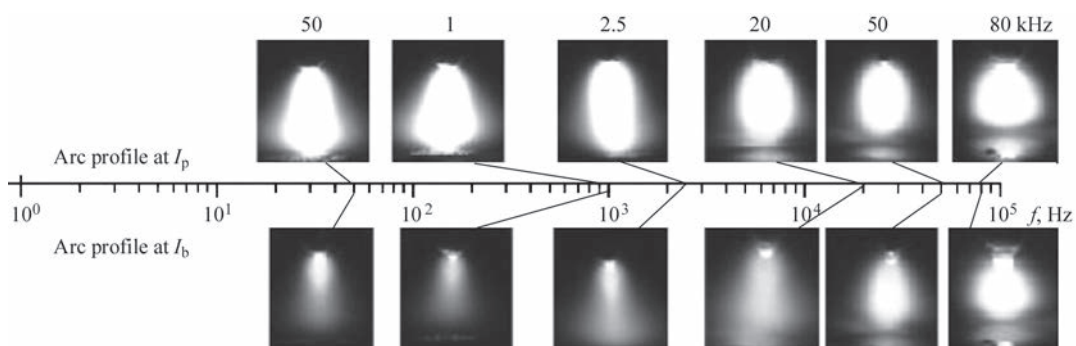


Figure 13. Appearance of the arc at $I = I_p$ (top) and at $I = I_b$ (below) for different values of current modulation frequency [15]

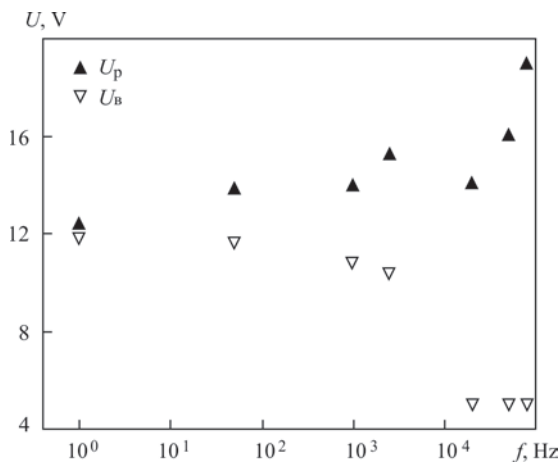


Figure 14. Dependencies of arc voltage in the pulse (1) and in the pause (2) on current modulation frequency [15]

value $U_b = U(I_b)$ on pulse modulation frequency are indicative of a significant increase of U_p and lowering of U_b with f increase, that qualitatively corresponds to the experimental data, given in [8] (see Figure 4). This leads to the arc voltage oscillating with ever increasing amplitude at increase of pulse modulation frequency.

Figure 15 gives the dependence of electron concentration N_e in arc column plasma at peak values of current on its modulation frequency. In order to find N_e the authors [15] used experimental data on widening of the spectral lines of arc plasma radiation due to Stark effect [35]. According to the obtained data, electron concentration in the arc column first grows with increase of current modulation frequency (right up to frequencies of the order of 20 kHz), and then drops abruptly. A possible cause for such behaviour of N_e is the fact that measurements of electron concentration were conducted near the anode, where plasma glow is markedly weaker at frequencies above 20 kHz, due to the change of arc column shape (see Figure 13).

In (17) the effect of current modulation frequency on arc characteristics was studied experimentally at TIG welding of aluminium alloy 5A06 3 mm thick

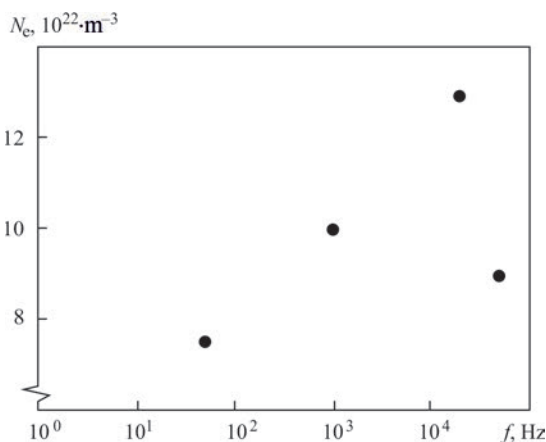


Figure 15. Dependence of electron concentration in the arc column at peak current values on its modulation frequency [15]

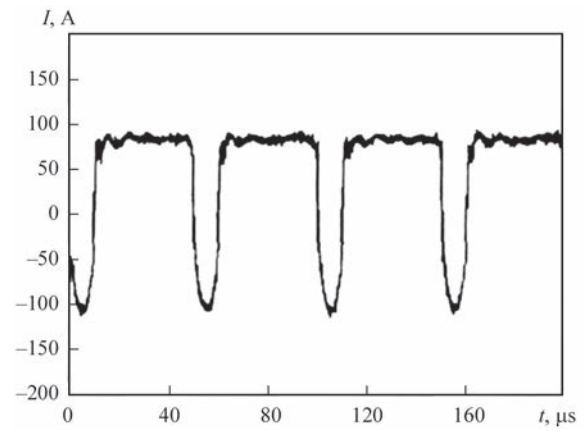


Figure 16. Dependence of arc current on time at TIG welding of an aluminium alloy in the mode of different polarity pulses [17]

in the mode of current pulses of different polarity. An arc of 3 mm length with tungsten cathode of 2.4 mm diameter was used in the experiments. Arc current was modulated by rectangular pulses (rate of current change at pulse fronts was equal to 50–100 A/μs) with amplitude of straight polarity current $I_p = 80$ A and of reverse polarity current $I_N = 120$ A at 8/2 ratio of durations of pulses of straight t_p and reverse t_N polarity. Modulation frequency f was varied in the range of 0.1–20 kHz. Oscillogram of welding current versus time at $f = 20$ kHz is given in Figure 16.

Respective oscillograms of arc current and voltage at $f = 5$ kHz are shown in Figure 17.

Figure 18 gives the measured values of arc voltage (during straight and reverse polarity of current), depending on modulation frequency. These experiments were performed using the following mode of current modulation: $I_p = 100$ A; $I_N = 120$ A; $t_p/t_N = 8/2$. As follows from Figure 18, arc voltage rises rather quickly with increase of modulation frequency in the range of $f < 1$ kHz, and at further frequency increase the rate of its rise drops markedly. Here, the voltage of straight polarity arc is essentially lower by absolute value than

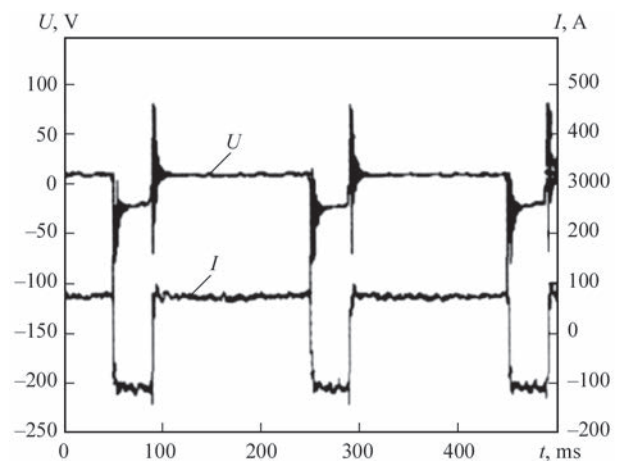


Figure 17. Oscillograms of voltage (upper curve) and current of the arc (lower curve) at TIG welding in the mode of different polarity pulses [17]

the respective value for reverse polarity arc in the entire studied frequency range.

Analysis of the results of experimental work, devoted to study of the peculiarities of physical phenomena, proceeding in nonstationary electric arcs in TIG welding with pulse modulation of welding current, leads to the following conclusions:

1. Shape of the luminous area of nonstationary arc column at TIG welding with high-frequency ($f > 10$ kHz) pulse modulation of current differs markedly from the respective shape for an arc of direct current, equal to average value of modulated current. This difference consists in a reduction of transverse dimensions (contraction) of the near-anode zone of the arc column, and, consequently, in increase of current density on the anode surface at increase of modulation frequency. As a result, the arc column shape changes from pear shape with diffuse binding to the anode at direct current to a spherical one with a dark space near the anode at HFP modulation of current. Here, for frequencies above 50 kHz the arc column shape during the current pulse practically does not differ from its respective shape during the pause.

2. High-frequency pulse modulation of current of an arc with a refractory cathode leads to an essential increase of the pressure of arc plasma flow on the anode surface, compared to DC arc pressure. At TIG welding with HFP modulation of current this causes an additional bending of weld pool surface, which results in lowering of the heat source into the metal being welded and, accordingly, increase of the arc penetrability. As regards the influence of current modulation frequency on arc pressure, this value grows rapidly with increase of frequency in medium frequency range ($f < 5$ kHz), whereas at further increase of modulation frequency by the data of different authors the arc pressure behaves differently: it somewhat decreases [10], stabilizes [13] or continues growing [14].

3. As regards the dependence of arc voltage on current modulation frequency in TIG welding, the authors of the considered works also have no consensus. So, for instance, by the data of [21–23] the effective value of voltage rises practically in proportion to modulation frequency. Experimental data of work [8] are indicative of the fact that the average value of arc voltage during the current pause decreases noticeably, whereas the average value of voltage during the pulse increases only slightly with frequency increase. As a result, both the average and effective values of arc voltage decrease with increase of current modulation frequency. Finally, in [15] it is shown that the arc voltage during the current pause decreases at increase of

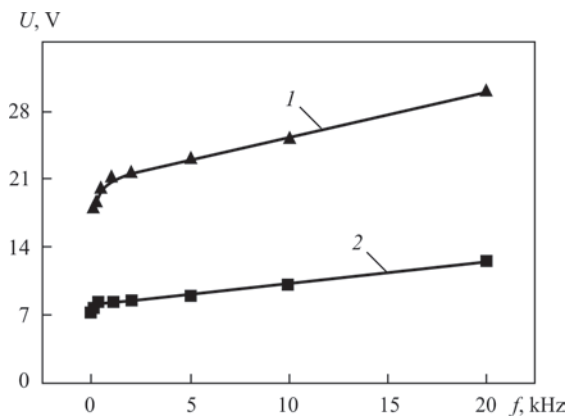


Figure 18. Dependence of absolute values of voltage of an arc of reverse (1) and straight (2) polarities at TIG welding in the mode of different polarity pulses on current modulation frequencies

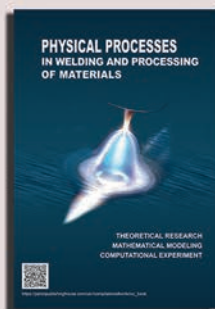
modulation frequency practically at the same rate, as the voltage during the pulse increases.

- Lienert, T.J., Babu, S.S., Siewert, T.A., Acoff, V.A. (2011) *ASM Handbook*. Vol. 6A. Welding fundamentals and processes. Ohio, USA, ASM International.
- Roden, W.A. (1972) High-frequency, pulsed-current GTA welding. In: *Proc. of National Aerospace Engineering and Manufacturing Meeting (2–5 Oct. 1972, San Diego, California, USA)*. Paper 720874, 1–8.
- Leitner, R.E., McElhinney, G.H., Pruitt, E.L. (1973) An investigation of pulsed GTA welding variables. *Welding J., Res. Suppl.*, **9**, 405–410.
- Yamamoto, T., Shimada, W., Gotoh, T. (1976) *Characteristics of high frequency pulsed DC TIG welding process*. Doc. IIW 212-628-76, 16–22.
- Sokolov, O.I., Gladkov, E.A. (1977) Dynamic characteristics of free-burning and constricted welding arc of direct current with nonconsumable electrode. *Svarochn. Proizvodstvo*, **4**, 3–5 [in Russian].
- Omar, A.A., Lundin, C.D. (1979) Pulsed plasma — pulsed GTA arcs: A study of the process variables. *Welding J., Res. Suppl.*, **4**, 97–105.
- Cook, G.E., Eassa, H.E.-D.E.H. (1985) The effect of high-frequency pulsing of a welding arc. *IEEE Transact. on Industrial Application*, 1A-21, **5**, 1294–1299.
- Kolasa, A., Matsunawa, A., Arata, Y. (1986) Dynamic characteristics of variable frequency pulsed TIG arc. *Transact. of JWRI*, **15**(2), 173–177.
- Saedi, H.R., Unkel, W. (1988) Arc and weld pool behavior for pulsed current GTAW. *Welding J., Res. Suppl.*, **11**, 247–255.
- Zhao, J., Sun, D., Hu, S. (1992) Arc behavior of high frequency pulse TIG welding arc. *Transact. China Weld Inst.*, **13**(1), 59–66.
- Kim, W.H., Na, S.J. (1998) Heat and fluid flow in pulsed current GTA weld pool. *Int. J. of Heat and Mass Transfer*, **41**(21), 3213–3227.
- Wu, C.S., Zheng, W., Wu, L. (1999) Modelling the transient behaviour of pulsed current tungsten-inert-gas weld pools. *Modelling and Simul. Mater. Sci. Eng.*, **7**(1), 15–23.
- Dzelnitzki, D. (2000) Muendersbach TIG — direct-current welding with high-frequency pulses, an interesting process variant. *EWM Hightec Welding GmbH*. 200. WM008801. DOC; 08.00.
- Onuki, J., Anazawa, Y., Nihei, M. et al. (2002) Development of a new high-frequency, high-peak current power source

- for high constricted arc formation. *Japan. J. Appl. Phys.*, **41**, 5821–5826.
15. Song, Y., Yan, S., Xiao, T. et al. (2010) A Study on the macro-micro physical properties in pulsed arc plasma. *Transact. of JWRI*, **39**(2), 17–18.
 16. Wu, C.S. (2008) *Welding heat process and pool geometry*. Beijing, China Machine Press, 102–104.
 17. Cong, B., Qi, B., Zhou, X. (2009) TIG arc behavior of ultrafast-convert high-frequency variable polarity square wave. *Transact. China Welding Institution*, **30**(6), 87–90.
 18. Traidia, A., Roger, F., Guyot, E. (2010) Optimal parameters for pulsed gas tungsten arc welding in partially and fully penetrated weld pools. *Int. J. of Thermal Sci.*, **49**, 1197–1208.
 19. Traidia, A., Roger, F. (2011) Numerical and experimental study of arc and weld pool behaviour for pulsed current GTA welding. *Int. J. of Heat and Mass Transfer.*, **54**, 2163–2179.
 20. Karunakaran, N., Balasubramanian, V. (2011) Effect of pulsed current on temperature distribution weld bead profiles and characteristics of gas tungsten arc welded aluminum alloy joints. *Transact. Nonferrous Met. Soc. China*, **21**, 278–286.
 21. Yang, M., Qi, B., Cong, B. et al. (2012) The influence of pulse current parameters on arc behavior by austenite stainless steel. *Transact. China Welding Institution*, **33**(10), 67–71.
 22. Qi, B., Yang, M., Cong, B. et al. (2012) Study on fast-convert ultrasonic frequency pulse TIG welding arc characteristic. *Mater. Sci. Forum.*, 704–705, 745–751.
 23. Qi, B., Yang, M., Cong, B. et al. (2013) The effect of arc behavior on weld geometry by high-frequency pulse GTAW process with 0Cr18Ni9Ti stainless steel. *Int. J. Adv. Manuf. Technol.*, **66**, 1545–1553.
 24. Yang, M., Qi, B., Cong, B. et al. (2013) Study on electromagnetic force in arc plasma with UHFP-GTAW of Ti–6Al–4V. *IEEE Transact. on Plasma Sci.*, **41**(9), 2561–2568.
 25. Yang, Z., Qi, B., Cong, B. et al. (2013) Effect of pulse frequency on weld appearance behavior by TC4 titanium alloys. *Transact. China Welding Institute*, **34**(12), 37–40.
 26. Krivtsun, I.V., Krikent, E.V., Demchenko, V.F. (2013) Modeling of dynamic characteristics of a pulsed arc with refractory cathode. *The Paton Welding J.*, **7**, 13–23.
 27. Yang, M., Yang, Z., Cong, B. et al. (2014) A study on the surface depression of the molten pool with pulsed welding. *Welding J., Res. Suppl.*, **93**(8), 312–319.
 28. Yang, M., Yang, Z., Qi, B. (2015) The effect of pulsed frequency on the plasma jet force with ultra high frequency pulsed arc welding. *IJW*, **8**, 875–882.
 29. Sydorets, V.N., Krivtsun, I.V., Demchenko, V.F. et al. (2016) Calculation and experimental research of static and dynamic volt-ampere characteristics of argon arc with refractory cathode. *The Paton Welding J.*, **2**, 2–8.
 30. Cunha ,T.V.d., Louise-Voigt ,A., Bohorquez, C.E.N. (2016) Analysis of mean and RMS current welding in the pulsed TIG welding process. *J. Materials Proc. Technology*, **231**, 449–455.
 31. Silva, D.C.C., Scotti, A. (2016) Using either Mean or RMS values to represent current in modeling of arc welding bead geometries. *Ibid.*, **240**, 382–387.
 32. Demchenko, V.F., Boi, U., Krivtsun, I.V., Shuba, I.V. (2017) Effective values of electrodynamic characteristics of the process of nonconsumable electrode welding with pulse modulation of arc current. *The Paton Welding J.*, **8**, 2–11.
 33. Nestor, O.H. (1962) Heat intensity and current density distributions at the anode of high current, inert gas arcs. *J. Appl. Phys.*, **33**(5), 1638–1648.
 34. Demchenko, V.F., Boi, U., Krivtsun, I.V. et al. (2016) Procedure of density distribution restoration of electric current in arc anode spot with refractory cathode according to experimental data obtained by the method of split anode. In: *Proc. of 8th Int. Conf. on Mathematical Modeling and Information Technologies in Welding and Related Processes (19–23 September 2016, Odessa Ukraine)*, 21–28.
 35. Grim, G. (1978) *Spectral line broadening in plasma*. Moscow, Mir [in Russian].

Received 28.10.2019

NEW BOOK



Physical processes in welding and material treatment. Theoretical investigation, mathematical modelling, numerical simulation collection of articles and reports: Collection of articles and reports edited by Prof. I.V. Krivtsun. Kyiv: International Association «Welding», 2018. — 642 p. ISBN 978-617-7015-74-0 (in Russian, English, Ukrainian).

The collection includes 86 papers and reports of research workers of the Department of physics of gas discharge and plasma technique at the E.O. Paton Electric Welding Institute of the NAS of Ukraine, being published in the period of 1978–2018. It generalizes the forty-year experience of research activity of the Department in the field of theoretical research and computer modelling of physical phenomena taking place in arc, plasma, laser and hybrid processes of welding, surfacing and coating deposition. It can be interesting and useful to the scientists, engineers and technologists dealing with the problems of arc, plasma, laser and hybrid welding and material treatment as well as post graduates and students studying theoretical basics of welding and related processes.

Orders for the collection, please send to the Editorial Board.

Collection in the open access:

https://patonpublishinghouse.com/compilations/Krivtsun_Sbornik_2018_small.pdf